

**ADVANCED REVIEW**

Next generation 3D pharmacophore modeling

David Schaller | Dora Šribar | Theresa Noonan | Lihua Deng |
 Trung Ngoc Nguyen | Szymon Pach | David Machalz |
 Marcel Bermudez | Gerhard Wolber

Pharmaceutical and Medicinal Chemistry,
 Freie Universität Berlin, Berlin, Germany

Correspondence

Marcel Bermudez and Gerhard Wolber,
 Pharmaceutical and Medicinal Chemistry,
 Freie Universität Berlin, Königin-Luise-
 Strasse 2+4, Berlin 14195, Germany.
 Email: m.bermudez@fu-berlin.de;
 gerhard.wolber@fu-berlin.de

Funding information

China Scholarship Council, Grant/Award
 Number: 201606010328; Deutsche
 Forschungsgemeinschaft, Grant/Award
 Number: 407626949; Deutscher
 Akademischer Austauschdienst;
 Sonnenfeld Foundation

Abstract

3D pharmacophore models are three-dimensional ensembles of chemically defined interactions of a ligand in its bioactive conformation. They represent an elegant way to decipher chemically encoded ligand information and have therefore become a valuable tool in drug design. In this review, we provide an overview on the basic concept of this method and summarize key studies for applying 3D pharmacophore models in virtual screening and mechanistic studies for protein functionality. Moreover, we discuss recent developments in the field. The combination of 3D pharmacophore models with molecular dynamics simulations could be a quantum leap forward since these approaches consider macromolecule–ligand interactions as dynamic and therefore show a physiologically relevant interaction pattern. Other trends include the efficient usage of 3D pharmacophore information in machine learning and artificial intelligence applications or freely accessible web servers for 3D pharmacophore modeling. The recent developments show that 3D pharmacophore modeling is a vibrant field with various applications in drug discovery and beyond.

This article is categorized under:

Computer and Information Science > Chemoinformatics

Computer and Information Science > Computer Algorithms and Programming

Molecular and Statistical Mechanics > Molecular Interactions

KEYWORDS

3D pharmacophores, artificial intelligence, machine learning, virtual screening, web services

1 | INTRODUCTION

Macromolecular biological structures such as proteins or DNA bind small organic molecules triggering functional modulation and biological response. The way in which ligands bind to their macromolecular targets is based on a small set of chemical interactions (chemical features), such as hydrogen bonds, charges, or lipophilic contacts. 3D pharmacophores represent

David Schaller, Dora Šribar, and Theresa Noonan contributed equally to this study.

This is an open access article under the terms of the Creative Commons Attribution License, which permits use, distribution and reproduction in any medium, provided the original work is properly cited.

© 2020 The Authors. *WIREs Computational Molecular Science* published by Wiley Periodicals, Inc.

an intuitive and powerful description of these interaction patterns. The high degree of abstraction in 3D pharmacophores enables the rationalization of binding modes for chemically diverse ligands and, subsequently, rapid and highly efficient virtual screening of molecular databases. Although the concept of 3D pharmacophores was developed at the beginning of the 19th century, virtual screening experiments were not performed until the late 80s and early 90s, when the first software packages for database searches were released.¹ The chemical space for molecules with a molecular weight below 500 Da is estimated to contain at least 10^{60} organic molecules.² Additionally, current developments in machine learning algorithms allow for *in silico* generation of billions of theoretically synthesizable molecules.³ 3D pharmacophores present a unique opportunity to harvest the enormous available chemical space for drug-like molecules.

In this review, we give a comprehensive overview of 3D pharmacophore models, their usage in drug design, and current developments in the field. We introduce the basic concept and summarize the underlying methodology for describing binding modes and for applying 3D pharmacophore models in virtual screening. We highlight the power of 3D pharmacophore models in drug discovery by showcasing key studies for virtual screening as well as studies that aim at a mechanistic understanding of protein functions. Moreover, we present and discuss current developments such as the integration of molecular dynamics, the combination with machine learning, and freely accessible web services.

2 | THE PRINCIPLES OF 3D PHARMACOPHORES

3D pharmacophores capture the nature and three-dimensional arrangement of chemical functionalities in ligands that are relevant for molecular interactions with the macromolecular target. Chemical functionalities are thereby classified into more general pharmacophore features, for example, hydrophobic areas, aromatic ring systems, hydrogen bond acceptors, hydrogen bond donors, negatively ionizable groups, and positively ionizable groups.⁴ Less common interaction types that contribute to the binding of ligands, such as metal coordination and halogen bonds, are either already implemented in most software packages or require user definition.^{5–7} Besides chemical nature and spatial arrangement, 3D pharmacophores can capture feature directionality in the case of hydrogen bonds and aromatic interactions.⁸ Additionally, spatial tolerance and weight can be fine-tuned for each pharmacophore feature to adjust its size and importance in the 3D pharmacophore. In order to describe the preferable shape of molecules in the binding site, pharmacophore features are often combined with exclusion volume constraints (also referred to as excluded volume constraints). For instance, an exclusion volume constraint may consist of a set of spheres that represent the protein residues imposing a barrier for binding of potential ligands.

Several 3D pharmacophore modeling programs have been developed, of which several are free for academic users (Table 1). Although the exact definition and implementation of pharmacophore features and their characteristics may differ between different 3D pharmacophore modeling programs, the underlying concept of 3D pharmacophores remains the same.

2.1 | 3D pharmacophore elucidation

3D pharmacophore elucidation methods can be classified as feature-based, substructure pattern-based, or molecular field-based, depending on how the pharmacophore features are derived. Feature-based methods derive pharmacophore features by filtering for geometric descriptors that match the characteristics of molecular interactions. Pattern-based methods, such as those implemented in PHASE, LigandScout, and Catalyst, detect substructures for chemical features in molecules. For example, all hydroxyl groups are defined as hydrogen bond donors and acceptors. In contrast, molecular field-based methods such as FLAP and Forge sample the molecular surface of either ligand or macromolecular target with different chemical probes and calculate interaction energy maps which can be translated into pharmacophore features. An additional distinction between 3D pharmacophore generation methods is based on the type of employed data. This could be a set of active ligands, structural data on the ligand in complex with its macromolecular target, or structural data of the macromolecular target alone (Figure 1).

2.1.1 | Ligand-based 3D pharmacophores

Ligand-based 3D pharmacophores are used when no structural information on the macromolecular target is available. They are composed of chemical features shared by a set of active compounds that are important for the interaction with

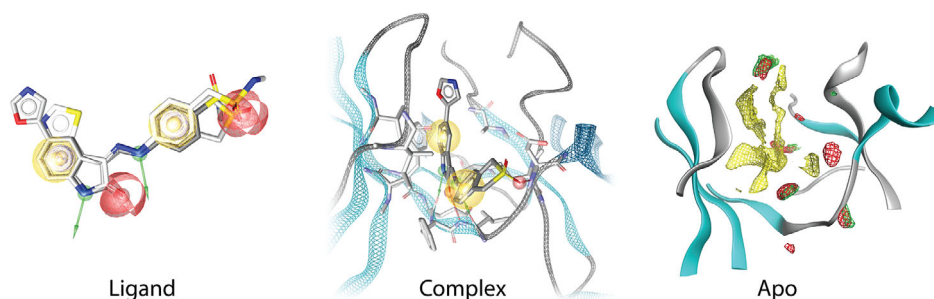
TABLE 1 3D pharmacophore modeling software, their components, and availability of free academic licenses

Software	Input	Identification methods	Virtual screening capability	Free for academic use ^a
FLAP ⁹	Ligand, complex, apo	Molecular field	Yes	No
Pharmer ¹⁰	Ligand, complex	Substructure pattern, feature	Yes	Yes (GPLv2)
LigandScout ¹¹	Ligand, complex, apo	Substructure pattern, feature, molecular field	Yes	No
Catalyst ¹²	Ligand, complex, apo	Substructure pattern, feature, molecular field	Yes	No
MOE ¹³	Ligand, complex, apo	Substructure pattern, feature, molecular field	Yes	No
PHASE ¹⁴	Ligand, complex, apo	Substructure pattern, feature, molecular field	Yes	No
Pharao ¹⁵	Ligand	Substructure pattern	Yes	Yes (GPLv2)
UNITY ¹⁶	Ligand, complex	Substructure pattern, feature	Yes	No
Forge ¹⁷	Ligand	Molecular field	Yes	Free for PhD students

Note: Software name describes virtual screening component. Names of 3D pharmacophore generation components in respective software suite may vary. 3D pharmacophores are commonly derived from an overlay of small molecules (ligand), from a ligand bound to its macromolecular target (complex) or from the macromolecular target alone (apo). Pharmacophore features are identified by analyzing molecular fields describing the potential interaction energy toward molecular probes (molecular field), by searching for substructure patterns able to perform the respective interaction (substructure pattern) or by filtering for geometric descriptors fulfilling the criteria for molecular interactions (feature).

^aThe software website was searched, or holder of rights was asked for academic license conditions.

FIGURE 1 3D pharmacophore generation approaches based on the available data. 3D pharmacophores can be generated from either a set of known ligands, atomistic models of ligand-macromolecular target complexes or the sole macromolecular (apo) target



the target (Figure 1). Shared pharmacophore features are usually derived from the 3D alignment of different conformations of active compounds. 3D structures of the conformers are aligned so that the same pharmacophoric features are located in similar positions. If all the aligned molecules share a certain feature at a specific position, a pharmacophoric feature is placed at this position.¹⁸ 3D alignments are often preceded by prefiltering steps based on quick distance checks, which substantially reduce computational time. For instance, the HipHop algorithm in Catalyst uses “pruned exhaustive search” and gradually builds-up shared 3D pharmacophores from the two-feature pharmacophores found in conformers of molecules.¹² In order to identify a shared 3D pharmacophore at each step, a precomputed list of all the interfeature distances in the molecule is first checked to see whether the specific feature combination is present. This prefiltering step is followed by alignment by least-squares fit of the features. LigandScout identifies optimal alignment by first checking best pairings between two sets of pharmacophore features based on interfeature distances, followed by alignment using the Kabsch algorithm.¹⁹ In some software packages, such as HypoGen in Catalyst, the derived three-dimensional arrangement of chemical features can be correlated with biological activities of known actives.^{14,20,21} This step can help to determine the importance of each feature for small molecule bioactivity.

However, it is important to note that bioactive conformations of the molecules are usually not known. Therefore, ligand-based 3D pharmacophore software considers a set of low energy conformations for each molecule. Although commercial conformer generation algorithms are generally successful in reproducing bioactive conformations, the ligand-based 3D pharmacophore generation procedure is not guaranteed to yield an alignment with the bioactive conformations.²² Another limitation of ligand-based 3D pharmacophores is the dependence on structurally similar molecules, since structurally more diverse molecules may not share the same binding mode and hence, require separate pharmacophore models. But even if different molecules share a common binding mode, a correct alignment becomes more challenging to the ligand-based algorithms the more diverse the molecules are.⁸

2.1.2 | Structure-based 3D pharmacophores

Structure-based 3D pharmacophore elucidation can be performed on atomistic models of two types of structures. In macromolecule–ligand complexes, a ligand is present in the binding site of the target molecule (Figure 1). Ligands in complex with a macromolecular structure are primarily either co-crystallized or docked into the target site. If there is no available structure of a macromolecule–ligand complex, or no known ligands at all for a binding site, programs can derive 3D pharmacophore models from atomistic models of apo structures (Figure 1; Table 1). These apo structures are atomistic models of macromolecules bound to no ligand.

Apo 3D pharmacophore elucidation techniques are especially useful in cases where there are no known ligands, necessitating a *de novo* approach to pharmacophore feature placement within the cavity. However, apo 3D pharmacophore generation methods can also be useful when applied to structures of macromolecule–ligand complexes. In this instance, they can be used to generate a novel 3D pharmacophore for the same active site that is unbiased by the existing ligand. This can be used to explore a novel region of chemical space for the same binding cavity. Accordingly, one of the strengths of 3D pharmacophore-based virtual screening is the potential for scaffold hopping afforded by the arrangement of abstract features not bound to any specific ligand structure.

Though they are the most common drug targets, proteins are not the only macromolecular structures analyzed in 3D pharmacophore development. Programs including LigandScout and Catalyst (Table 1) can generate 3D pharmacophore models based on nucleic acids. For example, Spitzer et al. generated a 3D pharmacophore hypothesis for minor groove binders based on a DNA–ligand complex.²³

Feature-based methods can be employed on macromolecule–ligand complexes as well as on empty binding sites. Feature-based programs analyze a target–ligand complex and employ a set of chemical and geometric rules to identify and classify target–ligand interactions, which then comprise the pharmacophore features.¹⁹ In an example of a feature-based method being applied to an apo structure, a strategy was developed by Schrödinger whereby fragments are docked into an apo binding site using the Glide XP docking program.^{24,25} The most energetically favorable fragment docking poses are selected to construct the 3D pharmacophore hypothesis using Phase (Table 1).¹⁴

Molecular field-based methods, such as FLAP (Table 1), employ molecular interaction fields (MIFs) to identify hotspots for pharmacophore feature placement.⁹ A prominent tool for generating MIFs is the GRID software, which is well known for its role in the discovery of the antiviral drug zanamivir.^{26,27} In principle, an evenly spaced grid is placed over a predefined binding cavity, and probes are placed to sample the binding site. These probes take the form of moieties representing the interactions most likely to occur between the macromolecule and ligand functional groups. As a next step, the energy between probe and target structure atom is calculated to define interaction sites. Thus, these probes can identify sites of favorable interactions with the macromolecule. These interaction energies generate MIFs, which are contoured by energy to generate maps that describe how the interaction energy between the target and a given probe varies over the surface of the target. Molecular field-based programs take the points where the energy of a MIF represents a local minimum, termed “hotspots,” and convert them into pharmacophore features according to the type of probe that forms the most energetically favorable interaction at this point. Molecular field-based hotspot detection can also be performed by employing noncommercial software such as AutoGrid within AutoDock which provides access to energy grid maps for various atom types.^{28,29}

Programs creating pharmacophore features for apo binding sites generate a surplus of possible features. These must be reduced to a reasonable number for virtual screening; a balance between enough features to allow for specificity, but not too many features, as this would be too restrictive and could lead to false negatives. Some programs include a feature reduction functionality, but other programs output an initial, unrefined 3D pharmacophore. The initial unrefined 3D pharmacophore composed of many features must then be reduced by the user. Feature selection can be based on information about the binding site and binding site-lining atoms, and according to which features of the binding site the user would like the ligands to exploit. Feature reduction must not only be performed manually; HS-Pharm³⁰ is an example of a program that uses machine learning to reduce the number of initial 3D pharmacophore features, as discussed in the advanced section later.

2.2 | Pharmacophore-based virtual screening

In pharmacophore-based virtual screening, 3D pharmacophores developed from either a set of active ligands, a target–ligand complex or the apo target, are screened against virtual libraries of molecules. Molecules that satisfy the query

pharmacophore requirements are retrieved from the libraries. The prioritization of compounds by virtual screening can dramatically increase the hit rate compared to in vitro high-throughput screenings and hence reduce the number of compounds for experimental testing (Figure 2).

To address conformational flexibility of the molecules, conformer libraries for the screened compounds are prepared before the screening step. It is worth mentioning that conformation generation is handled differently by screening software packages. Some software packages, such as LigandScout, Catalyst, or MOE perform virtual screening on a pre-generated set of conformations for each library molecule, while other software packages, such as PHASE, allow on-the-fly conformer generation during the screening step sacrificing virtual screening speed.^{19,31,32} For more information on conformer generation for virtual screening, the reader is encouraged to read available publications on this topic.^{8,22,32–36}

In the screening step, pharmacophoric features in the query pharmacophore are compared to pharmacophoric features present in the molecules of the screened library. Comparison methods can be divided into two distinct approaches: fingerprint-based and 3D alignment-based. Fingerprint-based methods, such as FLAP, primarily extract information about feature presence and/or interfeature geometries into fingerprint-like descriptors, which enables time-efficient similarity (e.g., using the Tanimoto coefficient) comparison between the query pharmacophore and the conformer library. Alignment-based methods including LigandScout, Catalyst, and PHASE perform 3D alignment of the pharmacophore feature set. A match is reported if the pharmacophoric feature set of a distinct conformation of a molecule can be aligned to the feature set of the query pharmacophore. 3D alignment is computationally expensive and time consuming, especially in the context of large molecular library screening. In order to reduce computational time, 3D alignment is often preceded by a fast prefiltering step based on feature-types, feature-counts, or fast distance checks.

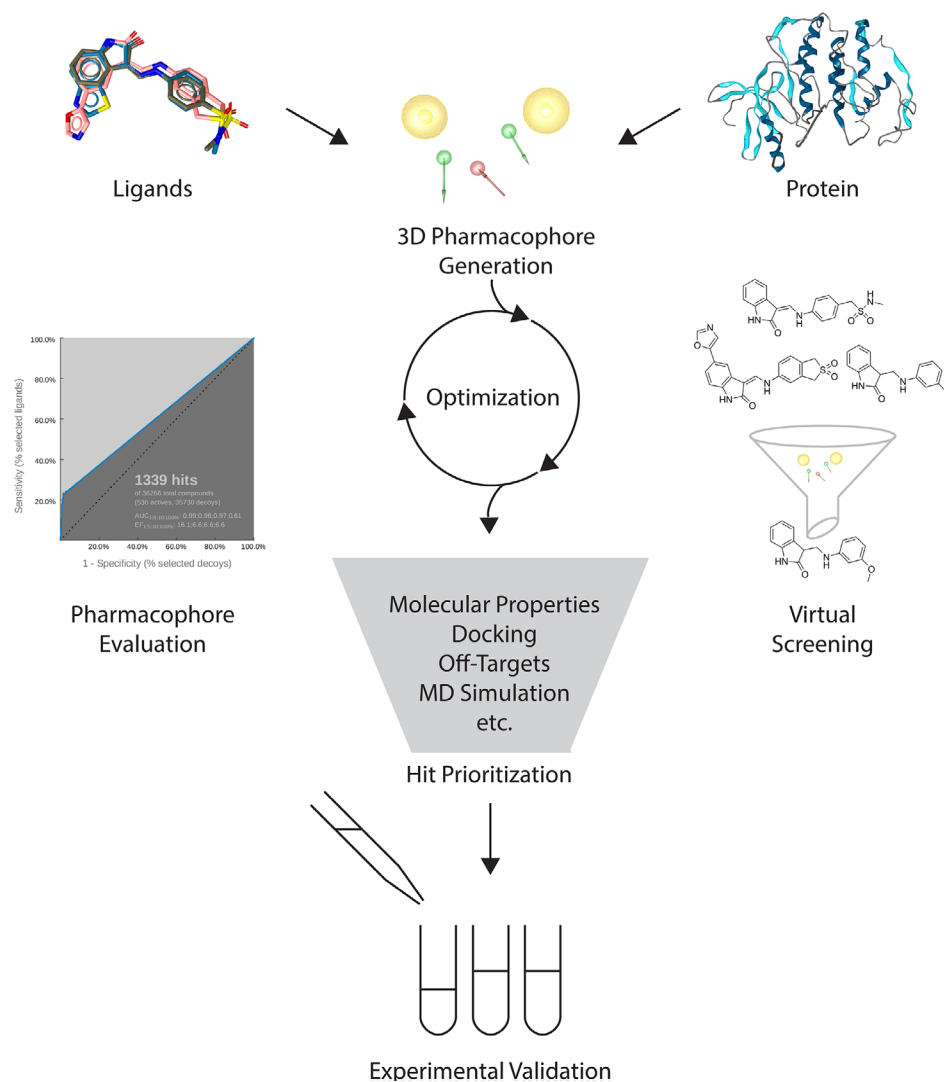


FIGURE 2 Virtual screening workflow. 3D pharmacophores are generated with either structure- or ligand-based approaches. State-of-the-art retrospective validation is performed by plotting ROC curves with elaborated sets of actives and decoys. Pharmacophore-based virtual screening is often followed by computationally more expensive methods such as docking or molecular dynamics simulations to get more differentiated structural insights. ROC, receiver operating characteristics

LigandScout is the only program that provides loss-less prefiltering steps, providing the most geometrically most accurate screening algorithm. Additionally, its unique pattern-matching 3D alignment algorithm results in screening hit lists that are orthogonal to other programs, mainly relying on interfeature distance fingerprints.³⁷

In cases where experimental data for binding ligands is available, derived 3D pharmacophore models can be validated. Usually, a validation set for 3D pharmacophores contains reported active, inactive and decoy molecules. Two points should be taken into consideration when preparing the validation set: Firstly, 3D pharmacophores describe a unique binding pose. Therefore, the active set should include molecules that share the same binding mode within the target protein. Secondly, reported inactives should be included with caution, as observed inactivity may result from other factors, for example, insolubility or inability to reach the target in cell-based assays. Therefore, the use of carefully selected decoys is encouraged over inactive molecules. A decoy is a compound presumed to be inactive and showing a high similarity in physicochemical properties to the active compounds. The Directory of Useful Decoys (DUD-E) provides a convenient web-based tool for the generation of decoys.³⁸ Subsequent screening against a validation set can be used to assess the quality of the developed 3D pharmacophore, and to further optimize it (Figure 2).

When evaluating the quality of a 3D pharmacophore model by its performance in virtual screening, various metrics, or enrichment parameters, are employed (Figure 2). 3D pharmacophore performance is evaluated in terms of how many actives the 3D pharmacophore can retrieve from a data set, and how well the 3D pharmacophore is able to correctly classify compounds as active or inactive. Enrichment parameters classify the compounds in the data set into one of four categories: active (true positive, TP); inactive but identified as active (false positive, FP); inactive (true negative, TN); active but classed as inactive (false negative, FN). Different metrics measure different aspects of 3D pharmacophore performance. These metrics include the yield of actives (YA), which describes the number of true positives present in the list of total hits retrieved by the 3D pharmacophore.³⁹ Receiver operating characteristics (ROC) curves plot the rate of true positives identified over the rate of false positives, thus displaying the sensitivity and specificity of the 3D pharmacophore model, characterizing how many active hits the 3D pharmacophore can identify in relation to how many inactive compounds it misidentifies as active.^{39–41} For a comprehensive list of enrichment parameters, how they are calculated, and their uses, the reader is referred to Braga and Andrade.⁴⁰

After a 3D pharmacophore has been developed and retrospectively validated, it can be used to screen available commercial or in-house compound libraries (Figure 2). Depending on the complexity of the 3D pharmacophore and the size of the library, hit lists of various sizes will be retrieved by pharmacophore screening. 3D pharmacophore-based screening is often followed by further characterization of the binding mode with methods like molecular docking, targeted molecular dynamics simulations, or other methods to gain more structural information to rationally prioritize molecules for experimental testing (Figure 2).

3 | APPLICATION CASE STUDIES

3.1 | Virtual screening

Besides molecular docking, 3D pharmacophores are widely applied for virtual screening. In this section, we highlight and discuss recent success stories of virtual screening campaigns covering different target classes and methodologies.

3.1.1 | Balancing the immune system with small molecule modulators

Toll-like receptors (TLRs) act as key players in the activation of the innate immune response by recognizing molecular patterns associated with infections and nonphysiological tissue damage.⁴² Rational design of small molecule TLR modulators is a promising strategy to treat autoimmune inflammation, cancer, or allergies, or to identify adjuvants for vaccines.⁴³

In 2014, Murgueitio and colleagues were facing a sparse data scenario with no small organic TLR2 inhibitors available.⁴⁴ Therefore, they generated a 3D pharmacophore based on MIFs to define key interactions necessary for ligand binding. A structure-based pharmacophore model was carefully developed. Subsequent virtual screening revealed novel antagonists in the low micromolar range with biological activity for 20% of their virtual hits. With more small organic TLR2 ligands reported later on, Murgueitio and colleagues continued their efforts in searching for novel TLR2

modulators and used a combined 3D pharmacophore and shape-based approach to discover a novel pyrogallol-based compound (MMG-11) through virtual screening.^{45,46}

In 2019, Šribar and co-workers conducted a structure-based virtual screening followed by in vitro experimental validation in seeking novel TLR8 modulators.⁴⁷ Molecular docking was performed to explore different binding modes able to explain the activity of known modulators. The most descriptive binding mode was translated into a 3D pharmacophore that was subsequently employed for virtual screening. This approach finally led to a novel chemotype for TLR8 inhibitors, where 36% of the molecules retrieved by this virtual screening approach showed activity in vitro.

3.1.2 | Discovery of novel covalent binding ligands

The design of covalent-binding ligands has gained increased popularity in the drug discovery community.^{48,49} Prolonged residence time on targets and pharmacodynamic effects independent from pharmacokinetics allow for lower doses or longer dosage intervals, making covalently binding drugs attractive for many therapies.^{50,51} Covalent docking and quantum mechanics (QM) calculations represent the “gold-standard” for the development of covalent binders.^{52,53} Docking is suitable for screening of small compound libraries, whereas QM calculations can be applied for single compounds only, due to high computational costs and time. For virtual screening of large databases, a pharmacophore-based approach is more applicable. Schulz and colleagues introduced a novel feature called “residue bonding point,” which recognizes drug-like warheads, such as ketones, nitriles, or Michael acceptors, to the LigandScout framework.^{11,54}

They employed the residue bonding point feature, also referred to as “covalent feature,” for the de novo design of viral 3C protease inhibitors.⁵⁴ A selective and specific 3D pharmacophore was generated that included noncovalent interactions crucial for substrate-recognition, as well as the novel covalent feature. The obtained 3D pharmacophore was used for virtual screening of a fragment library. Compounds showing a high similarity of docking poses in covalent and noncovalent form were selected for in vitro testing. Compound **F1**, a heterocyclic aromatic ketone, showed the highest inhibitory activity in an enzymatic assay (Figure 3). The covalent binding to the Cocksackievirus (CV) B3 protease was proven with protein mass spectrometry. Compound **F1** was optimized using a scaffold-hopping strategy, yielding in the more stable and active hit **C5**, a phenylthiomethyl ketone. This compound was modified using synthetic approaches to produce **7a**, a selective and irreversible covalent inhibitor of CV B3 and Enterovirus (EV) D68 protease. This example illustrates the ability of 3D pharmacophore models to not only identify novel ligands, but also their suitability for hit and lead optimization. Additionally, this study highlights the applicability of 3D pharmacophores for increasingly popular fragment-based drug discovery campaigns.⁵⁵

3.1.3 | Targeting GPCRs with 3D pharmacophores

G protein-coupled receptors (GPCR) are important drug targets due to their omnipresence in human tissues, accessibility to drugs, and regulatory roles in many physiological and pathophysiological processes.⁵⁶ Therefore, they are widely targeted by virtual screening campaigns in search of novel bioactive ligands.

In 2017, Frandsen and colleagues used an in-house developed method to build a histamine H3 receptor (H3R) pharmacophore model for virtual screening campaigns.⁵⁷ Ligand-residue fragments were extracted from available GPCR crystal structures and mapped to the same conserved binding pocket residues of the target receptor.⁵⁸ This method allows for structure-based modeling of orphan receptors with insufficient structural data or unknown ligands. Due to its reliance on existing ligand-receptor fragments from only 62 GPCR crystal structures, the initial H3R pharmacophore model missed an important cationic feature, which was added through docking studies and the matching of known H3R ligands to the apo pharmacophore model. Pharmacophore features were placed with Phase.¹⁴ Virtual screening, hit selection, and generation of analogue from potent ligands amounted to 76 compounds being pharmacologically tested with an IP1 accumulation and radioligand binding assay. Five neutral antagonists and one inverse agonist showed binding in the low micromolar range, resulting in a hit rate of 8%.

Another approach was followed by Schaller and co-workers using a ligand-guided homology modeling strategy to discover novel H3R ligands.⁵⁹ A key aspect of this approach is the prioritization of a set of 1,000 homology models based on their ability to explain the binding of nine known antagonists. The selected homology model was subsequently used for 3D pharmacophore model generation with LigandScout.¹¹ Complementarily, 10 diverse H3 receptor ligands were

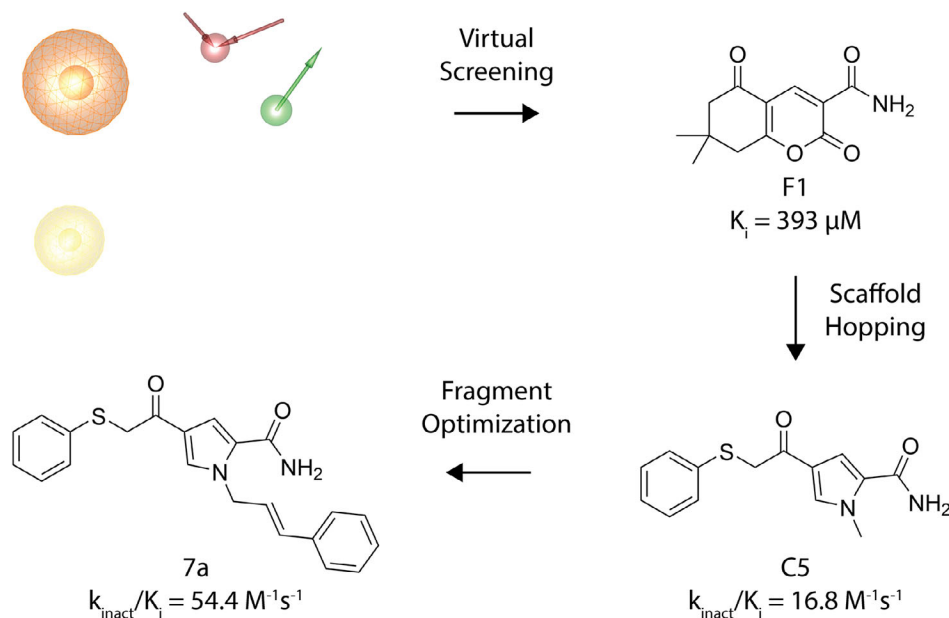


FIGURE 3 Discovery of covalent inhibitors of viral 3C protease. The initial fragment was identified with a 3D pharmacophore and further optimized by scaffold hopping and subsequent fragment growing. Green arrow—hydrogen bond donor, red arrow—hydrogen bond acceptor, yellow sphere—lipophilic contact, orange sphere—residue binding point

docked and evaluated by their interaction pattern. Resulting 3D pharmacophore models were iteratively optimized and validated with a set of 100 diverse active compounds and 3,051 decoys, using the three best performing 3D pharmacophore models for parallel virtual screening. Subsequently, eight hit molecules were selected for biological testing of which two showed nanomolar affinities in a radioligand depletion assay, resulting in a hit rate of 25%.

3.1.4 | Design of multitarget ligands for controlling inflammation

The arachidonic acid (AA) cascade is a key biochemical pathway for the inflammatory response involving the production of pro-inflammatory lipid mediators such as leukotrienes via 5-lipoxygenase-activating (FLA) protein, but also for anti-inflammatory mediators like epoxyeicosatrienoic acids. The latter are hydrolyzed by soluble epoxide hydrolase (sEH). The simultaneous inhibition of both enzymes therefore represents a promising approach for controlling inflammation mediators derived from AA. Schuster and co-workers applied a pharmacophore-based virtual screening to discover the first dual inhibitor of FLA protein and sHE with activities in the nanomolar range.⁶⁰ In a first step, they virtually screened the SPECS library with two different ligand-based pharmacophore models both derived from known FLA protein inhibitors. Twenty selected hit molecules were further prioritized by previously reported structure-based sHE models and resulted in one novel and potent dual FLA protein/sHE inhibitor.⁶¹ Since multitarget approaches are getting more and more attention, this example shows that ligand-based pharmacophores could have some benefits when applying on multiple targets that bind chemically similar physiological ligands. Moreover, it highlights the potential of combining ligand and structure-based models in multitarget approaches, in which one 3D pharmacophore serves as a prioritization tool for the hitlist derived by the other model.

3.1.5 | Design and optimization of novel agents in crop science

A successful application of ligand-based design in crop sciences was demonstrated by Yao et al. by targeting an enzyme in plant-pathogenic fungi.⁶² The group performed pharmacophore-based virtual screening to find inhibitors of succinate dehydrogenase (SDH). This protein is involved in the electron transport chain in eukaryotic mitochondria and represents a validated target for pesticides. All marketed SDH inhibitors consist of a carboxylate and amine-moiety coupled to an aromatic amide. Yao et al. generated a ligand-based 3D pharmacophore containing aromatic, lipophilic, and amide features applying Catalyst. The 3D pharmacophore was validated and used for a virtual screening campaign of a focused amide library developed in-house. To construct the focused amide library, diverse commercially available carboxylate moieties were linked to aniline using Discovery Studio's *Enumerate Library by Reaction* protocol to explore

the chemical space of carboxylate-cores. After virtual screening of the focused library, 16 compounds were selected for *in vivo* testing. Eight compounds showed more than 50% inhibition when tested against three different fungi species at a concentration of 100 mg/L. The ligand showing the highest and broadest activity was optimized via synthesis. In a second focused amide library, diverse amine moieties were linked to the best carboxylate core and screened against the 3D pharmacophore. The resulting collection of derivatives was tested *in vitro* on SDH. By combining *in silico* and experimental optimization steps, a broadly active novel amidic SDH inhibitor with low micromolar activity was developed.

3.2 | Understanding protein functionality

Besides describing ligand binding modes and virtual screening applications, 3D pharmacophores are powerful tools to investigate ligand-dependent protein functionality on a mechanistic level. The following paragraphs showcase examples where 3D pharmacophore models play an essential role in contributing to the mechanistic understanding of pharmacological effects.

3.2.1 | Modeling metabolism

Sulfotransferases (SULTs) play an important role in phase II metabolism, but represent challenging targets due to their high flexibility and broad substrate specificity. Rakers and colleagues developed a pharmacophore-based SULT prediction model to discriminate between substrates, inhibitors, and ligands that show both characteristics dependent on their concentration.⁶³ This study is remarkable for two reasons. Firstly, it uses an ensemble of different enzyme conformations derived from molecular dynamics (MD) simulations to generate conformation-specific 3D pharmacophore models. Secondly, the pharmacophore fit score was incorporated into a machine learning approach based on support-vector machines for post-filtering of screening results. The resulting pharmacophore-based prediction model was successfully applied to the screening and classification of ligand types for SULT1E1 and enhances our understanding of SULT enzyme specificity.

The aryl hydrocarbon receptor (AHR) is a ligand-dependent transcription factor controlling the metabolism of physiological substances and xenobiotics. Based on carefully validated homology models, Tkachenko and colleagues applied 3D pharmacophore models to study differences between physiological ligands and xenobiotics with regard to AHR transport to the nucleus and subsequent induction of CYP1A1.⁶⁴ Histidine 291 was identified as a key residue, which controls both functionalities, but with different roles in binding of physiological ligands such as kynurenine and xenobiotics such as β -naphthoflavone.

3.2.2 | Investigating ligand-dependent receptor function

GPCRs represent an important drug target class with highly complex pharmacology and various possibilities to modulate receptor function in a ligand-dependent manner. One major issue in this field is receptor selectivity, especially for closely related subtypes of the same family. In order to understand subtype selectivity of bitopic (dualsteric) ligands at muscarinic receptors, Bermudez and co-workers used 3D pharmacophore models to identify subtype-specific interaction patterns.⁶⁵ This rationally explained, on the one hand, how ligands achieve selectivity for a certain subtype, and, on the other, identified key residues in the extracellular loop regions (e.g., a M3-specific salt bridge) that account for subtype-specific receptor functionality. Some of the aforementioned bitopic ligands for the M2 receptor showed some unexpected yet interesting pharmacological properties, such as partial agonism and pathway-specific receptor activation (biased signaling). In order to understand these effects, 3D pharmacophore models were combined with other modeling techniques and pharmacological experiments.^{66,67} The partial agonism could be explained by the existence of multiple binding modes, which stabilize different activation states of the receptor. This concept was validated by experiments and resulted in the rational design of a full agonist, which can only adopt the binding mode stabilizing active receptor states.⁶⁶ The pathway-specificity of the biased ligands was studied in a similar setting and resulted in a mechanistic model whose key concept resides in the conformational restriction of the extracellular loop region.^{67–69} In another study, the effect of fluorination of the photoswitchable azobenzene core was investigated in muscarinic agonists. This

study shows that fluorination of the photoswitch alters not only the photochromic behavior but also the pharmacological profile at the M1 receptor, due to additional interaction possibilities.⁷⁰ In all of these GPCR studies, 3D pharmacophores were key to understanding ligand-dependent receptor functions and, moreover, turned out to serve as the optimal instrument for communication with synthetic chemists and pharmacologists.

4 | ADVANCED APPROACHES EMPLOYING 3D PHARMACOPHORE PRINCIPLES

In the previous sections, we gave an overview of the concept of 3D pharmacophores and on which established software is available. Additionally, we presented several state-of-the-art application case studies employing 3D pharmacophores for prospective virtual screening and for understanding protein functionality. But what could be considered an advanced approach? Typically, 3D pharmacophores are generated from atomistic models of macromolecules or from an alignment of multiple ligand conformations and are employed for analysis of structure–activity relationships or virtual screening campaigns. Moreover, a local installation of software and the availability of a high-performance computer are usually mandatory to perform virtual screening experiments. In the following section, we introduce advanced approaches that integrate conformations from MD simulations, employ machine learning algorithms, and provide access to 3D pharmacophore searches without the requirement of expensive licenses and high-performance computers (Table 2).

4.1 | Integration of information from molecular dynamics simulations

Since both macromolecules and ligands are dynamic entities, it becomes apparent that this also holds true for macromolecule–ligand complexes and the underlying interactions. Following this idea, Carlson and colleagues integrated information from MD simulations in the development of an enhanced 3D pharmacophore model to virtually screen for novel HIV-1 integrase inhibitors.⁹² Later, Carlson used the HIV-1 protease to show that a 3D pharmacophore generated from an ensemble of 28 NMR conformations performs better than a 3D pharmacophore generated from 90 X-ray structures.⁹³ This pioneering work inspired other researchers and kick-started the development of several methods employing conformations from MD simulations for 3D pharmacophore generation.

Hydration-site-restricted pharmacophore (2012). Unrefined 3D pharmacophore models generated from apo binding cavities usually contain too many features for efficient virtual screening. The hydration-site-restricted pharmacophore (HSRP) approach aims at reducing the number of pharmacophore features by identifying hydration sites on the protein surface, whose water molecules suffer from unfavorable thermodynamic properties as calculated from MD simulations.⁷¹ These restricted 3D pharmacophores also should be more likely to retrieve entropically favorable ligands. The HSRP approach was evaluated for three pharmaceutically relevant target proteins, showing a successful reduction of pharmacophore feature space with a simultaneous decrease in required computing power.

SILCS-Pharm (2014). SILCS-Pharm exploits binding hotspots of probe molecules in MD simulations for 3D pharmacophore generation.^{72,73} The SILCS (site identification by ligand competitive saturation) method is employed to sample the surface of proteins in MD simulations with different probe molecules reassembling properties known from pharmacophore features, for example, benzene carbons for aromatic features.⁹⁴ The resulting probability maps of the different probe molecules (FragMaps) are Boltzmann-transformed into free energy representations. These free energy FragMaps are finally converted to pharmacophore features and the associated free energies can be used to prioritize feature selection in 3D pharmacophore model generation. The authors showed that 3D pharmacophores generated with SILCS-Pharm often perform better than various docking approaches and 3D pharmacophores generated with the HSRP method described above. SILCS-Pharm was already employed in guiding binding pose predictions of novel inhibitors targeting the oncoproteins Mcl-1 and Bcl-xL.⁹⁵

Dynophores (dynamic pharmacophores) (2015). Contrary to approaches that gather pharmacophore information from ensembles of different protein conformations based on MD, the dynophore app represents a fully automated implementation of chemical feature-based interaction patterns with MD-based conformational sampling.^{66,74} Dynophores (dynamic pharmacophores) sequentially extract interaction points (such as hydrogen bonds, charges, or lipophilic contacts) from each frame of a trajectory according to the ligand atoms involved and their feature type. The resulting super-features can be statistically characterized by occurrence frequency and interaction patterns with the

TABLE 2 Advanced approaches employing the 3D pharmacophore concept

Category	Approach	Description
MD integration	Hydration-site restricted pharmacophore ⁷¹	Thermodynamic properties of water molecules are used to reduce the number of features in apo-based 3D pharmacophore models
	SILCS-Pharm ^{72,73}	Binding hot spots of probe molecules in MD simulations are exploited for 3D pharmacophore generation
	Dynophore ⁷⁴	Fully automated combination of 3D pharmacophores and MD simulations with statistics on spatiotemporal feature occurrence
	Common hits approach ⁷⁵	3D pharmacophore models from MD simulations are grouped according to interaction pattern and used for parallel screening
	MYSHAPE ⁷⁶	Interaction patterns in MD simulations are analyzed to refine shared-feature pharmacophores
	GRAIL ⁷⁷	Molecular interaction fields are abstracted to the pharmacophoric level and averaged over an MD simulation
	Water pharmacophore ⁷⁸	Water thermodynamics, docking, and molecular interaction fields are used to generate a single 3D pharmacophore model
	PyRod ⁷⁹	Protein environment of water molecules is analyzed to generate dynamic molecular interaction fields for visualization and 3D pharmacophores for virtual screening
	AutoDock Bias ⁸⁰	Cosolvent simulations are used to bias a docking algorithm
Machine learning	Pharmmaker ⁸¹	Cosolvent simulations are analyzed to generate 3D pharmacophores for virtual screening
	HSPHarm ³⁰	Random forest decision tree is trained on pharmacophoric fingerprints to reduce the number of features in apo-based 3D pharmacophore models
	PharmIF ⁸²	Support vector machine is trained on pharmacophoric fingerprints to rank docking poses
Web applications	DeepSite and related softwares ^{83–86}	Convolutional neural network is trained on pharmacophoric descriptors to detect cavities, predict binding affinities, and to design new molecules
	PharmaGist ⁸⁷	Ligand-based 3D pharmacophore generation
	PharmMapper ⁸⁸	Target prediction of small molecules employing a database of 3D pharmacophores
	Pharmer related applications ^{89–91}	3D pharmacophore generation and virtual screening of small molecule databases

protein. Three-dimensional volumetric feature density clouds provide information about the spatial distribution of interactions and barcode plots show the feature occurrence in a time-resolved manner. The dynophore app was implemented within the ilib/LigandScout framework¹¹ and addresses two shortcomings of classical 3D pharmacophore models: their static character and the geometric simplification of the features.

The application of dynophores proved essential in several studies for rationally explaining phenomena which could not have been unveiled by classical 3D pharmacophores alone. Dynophores were first used to explain an activity cliff of two ligands at the M₂ receptor, which differ in structure by a single double bond (dihydroisoxazole vs. isoxazole moiety) and therefore show the same static 3D pharmacophore.⁶⁶ Based on the occurrence frequency and the respective geometric properties of a hydrogen bond acceptor, different strengths of the resulting hydrogen bond between the two ligands could be rationalized. In another example, dynophores were able to unveil a mechanism to overcome drug resistance for HIV-1 reverse transcriptase (RT). In this study, the RT inhibitor rilpivirine was shown to bypass resistance mutations by interacting with alternate residues, stabilizing the inhibitor in the binding pocket.⁹⁶ In a virtual screening campaign against the metalloenzyme arginase, dynophores were employed to explore the plasticity of the binding pocket in the presence of small molecule inhibitors and suggested the possibility for additional lipophilic contacts. This resulted in two novel fragment arginase inhibitors that could aid the development of anticancer drugs.⁹⁷ The dynophore methodology enables researchers to escape the static nature of classical 3D pharmacophore approaches and provides

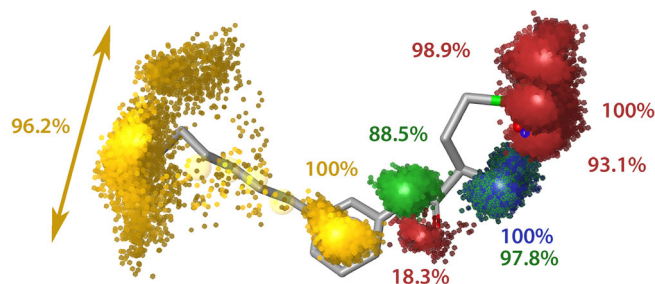


FIGURE 4 Dynophores (dynamic pharmacophores) unveil dynamic binding mode changes of the sphingosine-1-phosphate receptor ligand ML056 during a 100 ns MD simulation. The yellow point clouds indicate lipophilic contacts, the red and green features represent hydrogen bond acceptor or donor, respectively, and a positively charged area is shown as a blue point cloud. The percentages next to the features refer to their occurrence frequency during the simulation. In the example shown, a major part of the molecule remains in its initial orientation resulting in nearly sphere-like distributions of the according feature point clouds (right part). The lipophilic tail is much more flexible within the binding site as indicated by the banana-shaped feature cloud (left part). MD, molecular dynamics

new opportunities to describe and analyze ligand binding modes as dynamic events (Figure 4).^{47,66,96–101} The probability density functions representing the feature distribution of the super-features can be directly used for virtual screening, providing new possibilities for efficiently incorporating information from molecular dynamics simulations into fast and efficient virtual screening.

Common hits approach and MYSHAPE (2017). These two approaches select and optimize 3D pharmacophores based on MD simulations. The Common Hits Approach (CHA) groups 3D pharmacophore models obtained from protein–ligand conformations of MD simulations according to their interaction pattern.⁷⁵ Representative 3D pharmacophores are subsequently used for computationally costly virtual screening. CHA was retrospectively evaluated on 40 protein–ligand systems, showing improved virtual screening performance for many of the protein–ligand complexes compared to the use of single 3D pharmacophore models. In contrast, MYSHAPE optimizes shared-feature pharmacophores by focusing on pharmacophore features observed during MD simulations of different protein–ligand complexes. This approach was found in a retrospective evaluation against PPAR α to perform better than 3D pharmacophores derived from X-ray structure.⁷⁶

GRAIL (2018). The GRids of pharmacophore Interaction fieLds (GRAIL) approach depicts MIFs on the pharmacophore level in MD simulations.⁷⁷ Beside pharmacophoric interaction fields, this approach generates information on atom densities for protein, water, and ligand if present. GRAIL was applied to MD simulations of heat shock protein 90 showing that the pharmacophoric interaction fields can contribute to the understanding of the structure–activity relationship of a complexed ligand series.

Water pharmacophore (2018). The Water Pharmacophore (WP) method aims at generating 3D pharmacophores based on thermodynamic properties of hydration sites, similar to the HSPR approach described above.^{71,78} WPs are generated for hydration sites by a combination of thermodynamic analysis, MIFs, and docking-based strategies. However, in contrast to HSPR, the WP method generates a single 3D pharmacophore in a highly automated fashion with a comparably low number of involved features granting high performance in virtual screening campaigns. After optimizing parameters for the 3D pharmacophore generation procedure against seven pharmaceutically relevant targets, the authors were able to generate successful 3D pharmacophores for four out of seven targets.

PyRod (2019). Similar to WP and HSRP, the free and open-source software PyRod focuses on water molecules in protein binding pockets to generate 3D pharmacophores for virtual screening.⁷⁹ However, instead of determining thermodynamic properties of hydration sites, PyRod analyzes the protein environment of water molecules in protein binding pockets based on fast-to-calculate pharmacophore inspired heuristic scoring functions. This information is further processed to visualize pharmacophoric binding pocket characteristics in the form of dynamic dMIFs and to generate pharmacophore features for virtual screening (Figure 5). Since scoring is only performed in the presence of water molecules, pharmacophore features are preferentially placed at hydration sites with high water occupancy. Replacing such water molecules with a ligand moiety results in a gain of entropy and hence increases the chance for discovery of high affinity ligands. Similar to other apo-based pharmacophore methods, the unrefined 3D pharmacophore contains too many features for efficient virtual screening. Hence, the user must first preselect pharmacophore features based on dMIFs and their arrangement in the binding pocket. The features of this focused 3D pharmacophore are subsequently combined to generate a pharmacophore library based on user-defined characteristics, for example, maximal and

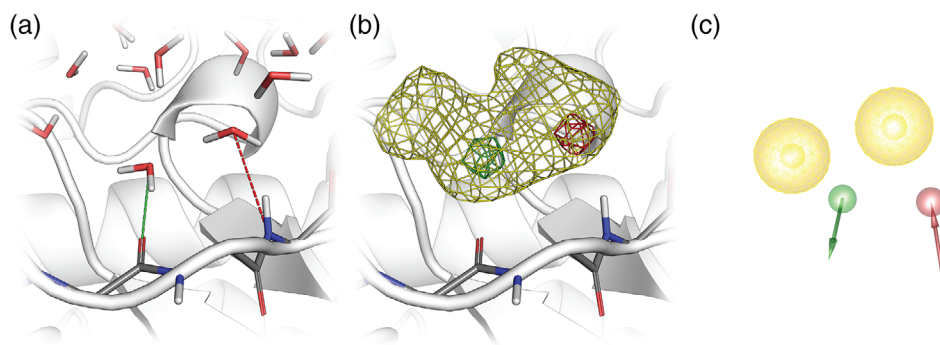


FIGURE 5 PyRod applied to the binding pocket of cyclin-dependent kinase 2. (a) The protein environment of water molecules is analyzed to generate (b) dynamic molecular interaction fields (DMIFs) describing the pharmacophoric characteristics of the binding pocket, (c) which can be translated into pharmacophore features for virtual screening. Yellow—hydrophobic contact, green—hydrogen bond donor, red—hydrogen bond acceptor

minimal number of independent features or hydrophobic contacts. A Python script is provided allowing for evaluation of the generated pharmacophore library using LigandScout.¹¹ PyRod pharmacophores performed better than docking for three out of five pharmaceutically relevant targets, according to ROC analysis in a retrospective evaluation and provides a directly usable workflow for efficient virtual screening.

AutoDock Bias with Solvent Sites (2019) employs cosolvent based pharmacophores to bias docking algorithms toward hotspots of probe molecule binding for improving virtual screening performance.^{80,102,103} First, the authors performed cosolvent MD simulations of proteins in the presence of water and ethanol. Next, the trajectories were analyzed to identify hotspots for binding of the ethanol hydroxyl- and methyl-group. Finally, the calculated free energies of ethanol hotspots were used to introduce an additional energy term to the docking algorithm of AutoDock 4.^{28,80} The biased docking performance was retrospectively evaluated, showing improved performance compared to the standard docking procedure in the majority of investigated test systems.¹⁰³

Pharmmaker (2020) analyzes cosolvent simulations to generate 3D Pharmacophores for virtual screening.⁸¹ In the presented case study, cosolvent simulations were performed using six different probe molecules and subsequently employed to assess the druggability of different binding sites with DruGUI.¹⁰⁴ The most druggable binding site was subsequently processed with Pharmmaker by selecting protein residues with high probe-specific affinities and by identifying snapshots that show the most frequent interactions between protein residues and probe molecules. Finally, 3D pharmacophores were generated from selected snapshots and employed for virtual screening with Pharmit,⁸⁹ a web application for pharmacophore screening described later in this review.

In addition to 3D pharmacophore modeling, the benefit of multiple protein conformations in enhancing the performance of molecular docking is also frequently discussed.¹⁰⁵ However, ensemble docking in multiple X-ray structures revealed minor improvements in screening performance in only some test systems, which hardly justifies the increased computational costs.¹⁰⁶ Clustering protein conformations could be a solution to reduce the computational costs, but fails to identify the most relevant protein conformations from MD simulations.¹⁰⁷ In contrast to molecular docking, the presented 3D pharmacophore approaches show clear advantages over traditional static pharmacophore modeling. Dynophores, for example, provide a statistical characterization of interactions in the form of volumetric feature density clouds. Escaping from the spherical nature of traditional pharmacophore features in conjunction with the representation of pharmacophore features as probability density functions represents a strong opportunity to boost virtual screening performance. Furthermore, approaches like PyRod consider entropic contribution of ligand binding which can only be poorly estimated by static methods. In comparison to these advanced pharmacophore approaches, ensemble docking represents a computationally expensive parallelization of the same underlying algorithms. Hence, important information contained in MD simulations is not properly considered, resulting in comparably poor improvement of performance.

4.2 | Training machine learning models with pharmacophoric descriptors

In recent years, machine learning and artificial intelligence have witnessed tremendous amount of attention in the public media. The simultaneous improvement in computing power and increase of available data have heavily influenced

the modern drug discovery process.¹⁰⁸ Moreover, the concept of 3D pharmacophores was employed to develop several new machine learning methods.

HS-pharm (2008). The Hot-Spots-Guided Receptor-Based Pharmacophores (HS-Pharm) approach trains machine learning models to reduce the number of features from apo-based 3D pharmacophore models.³⁰ The binding cavities of ~3,500 resolved protein–ligand complexes were analyzed and over 600 k atoms were distributed into interacting and noninteracting groups. Atom-based cavity fingerprints were generated from the gathered cavity atoms, collecting data about pharmacophoric and torsional properties, involved residues, and their protein environment. Decision trees and Bayesian classifiers were trained and tested on these fingerprints to detect cavity atoms important for ligand binding. Evaluation of the approach identified random forest decision trees to perform best according to enrichment and ROC analysis. Finally, this approach was applied to three pharmaceutical relevant drug targets resulting in the generation of 3D pharmacophores performing better than docking in two out of three cases.

Pharm-IF (2010). The pharmacophore-based interaction fingerprint Pharm-IF was evaluated as input for several machine learning algorithms to rank docking poses of small molecules.⁸² Interaction fingerprints encoding the type and distance of interaction partners were generated for all available atomistic models of five pharmaceutically relevant drug targets. These were subsequently used to train several machine learning algorithms to rank docking poses of known actives and decoys. In a retrospective evaluation, Pharm-IF fingerprints in combination with support-vector machines showed the best enrichment, outperforming other machine learning algorithms and a docking scoring function. Employing Pharm-IF to train machine learning algorithms resulted in better enrichment compared to employing PLIF, a protein–ligand interaction fingerprint implemented in MOE.¹³ In contrast to Pharm-IF, this fingerprint does not encode the distance, which suggests an important contribution of the distance to successful predictions. Interestingly, learning on more than five crystal structures enabled models to predict activity better than docking scores for all studied targets.

DeepSite and related softwares (2017). The DeepSite software employs convolutional neural networks typically used for analyzing visual imagery to predict the druggability of protein binding pockets.⁸³ Atomic-based pharmacophoric descriptors were assigned to grid points covering the protein of approximately 7,000 protein–ligand complexes. These grids were subsequently divided into subgrids, which were labeled as a binding site if their geometric center was within 4 Å of the binding site's geometric center. These 3D images of the binding pocket represented by 3D grids of pharmacophoric descriptors were used to train a convolutional neural network. The DeepSite cavity detection was found to perform better than other state-of-the-art detection algorithms. Similar approaches that also use pharmacophoric descriptors to train convolutional neural networks were later used to predict binding affinities of small molecules (K_{DEEP} ⁸⁴) and to guide the design of novel molecules (LigVoxel,⁸⁵ LigDream⁸⁶). All of the aforementioned approaches are implemented in software packages for local installation but can also be used free of charge as web applications.

4.3 | Web applications employing 3D pharmacophores

Although web applications do not necessarily represent an advancement of the 3D pharmacophore concept itself, they do advance their usability, bringing 3D pharmacophores into the internet age. Since a local installation of software is not needed and all web applications presented are freely available for academic research, users can circumvent license fees and screen databases with millions of molecules without the need for high-performance computational resources. Thus, 3D pharmacophore searches become available to a larger number of users.

PharmaGist (2008). The PharmaGist web application allows for ligand-based 3D pharmacophore generation.⁸⁷ Each submitted ligand is analyzed for rotatable bonds important for flexible molecule alignment and for pharmacophoric features used for alignment to a reference ligand. A user-specified maximal number of 3D pharmacophores is generated, and the output comprising 3D pharmacophores and aligned molecules can be downloaded.

PharmMapper (2010). The PharmMapper web application can be used for target fishing of small molecules important for off-target prediction and polypharmacology studies.⁸⁸ More than 53,000 3D pharmacophore models were generated from approximately 23,000 protein database (PDB) crystal structures based on protein–ligand interactions or involving a cavity detection algorithm to identify potential allosteric binding sites. Submitted molecules are scored by their match to all deposited 3D pharmacophore models.

Pharmer-based web applications (2012). The Pharmer virtual screening software¹⁰ was employed for several web applications enabling the efficient virtual screening of several small molecule databases. AnchorQuery is specialized for

the identification of protein–protein interaction inhibitors.⁹⁰ The user uploads a protein–protein complex and specifies an anchor residue that is likely to be important for protein–protein interaction. This anchor residue will become part of a 3D pharmacophore that is used to screen a multimillion compound library of synthesizable small molecules. ZINCPharmer can be used to perform a virtual screening of the ZINC database, a free virtual library collecting commercially available compounds from different vendors.^{91,109} The web application supports the import of 3D pharmacophores but can also be used to generate 3D pharmacophore models from scratch. Lastly, Pharmit enables the virtual screening of several commercial vendors as well as other noncommercial databases including ChEMBL and PubChem.^{89,110,111} The 3D pharmacophores can be either designed from a protein–ligand complex or, a ligand. The import of 3D pharmacophore models in several data formats is also supported.

5 | CONCLUSION

In this review, we have given an overview of the principles of 3D pharmacophores and their role in drug discovery. The fact that 3D pharmacophore models are universal, editable, and comprehensive allows them to be applied in different scenarios.

A major application field is the identification of novel ligands through virtual screening. For this purpose, 3D pharmacophore models are the sole technique that can be applied in either a ligand-based or a structure-based manner. In both ways, 3D pharmacophore models are computationally very efficient, enabling the virtual screening of very large databases. The basic concept of abstracting chemical functionality allows for scaffold hopping and enriches the chemical diversity of hit lists. Altogether, this grants researchers more flexibility regarding available data, computational resources, and testing capabilities. The case studies that we selected highlight the power of pharmacophore-based virtual screening for drug discovery and show their applicability to challenging targets. Also, increasingly popular fragment-based drug discovery campaigns can benefit from pharmacophore screening by a dramatic reduction of fragments tested *in vitro* and by rationalizing fragment growing with constant fragment core interactions.^{54,55}

Besides virtual screening, 3D pharmacophores are well suited to study and visualize binding modes of drug-like molecules. Their composition of a limited number of chemically defined interaction features make them understandable and intuitive. This represents a major advantage in interdisciplinary projects, since 3D pharmacophore models are able to rationalize various pharmacological effects. For this objective, 3D pharmacophores are typically combined with other methods such as docking, MD simulations, or machine learning. The selected case studies for this field underline the power of 3D pharmacophores to mechanistically explain and understand protein functionality. Additionally, 3D pharmacophores are an excellent tool for communication between researchers, a factor that is often underestimated.

However, besides the aforementioned advantages and possibilities, classic 3D pharmacophore models also have certain drawbacks. They represent static models for highly dynamic systems and their interaction features are restricted to simple geometries (e.g., spherical features). Moreover, they share a shortcoming with other modeling techniques, which all are focused on estimating the enthalpy of molecular interactions but are suboptimal for the description of entropic effects. However, enthalpy and entropy both contribute to the change in free energy of ligand binding to a macromolecule. Although the basic concept of 3D pharmacophore generation and its application to virtual screening has not changed in the last 30 years, there are various developments in the field that aim at addressing these shortcomings.

The combination of 3D pharmacophore models with MDs is therefore a consequent evolution with great potential. Different approaches to integrating MDs into 3D pharmacophore modeling have been reported and described in this review.^{71–75,77–79,81,103} However, only the dynophore method represents a fully automated approach, which tackles two drawbacks of classical 3D pharmacophores at a time.⁷⁴ The dynophore application reveals a new perspective on ligand binding by providing visualization of pharmacophoric features that escape from the traditional spherical geometry and by delivering statistics that report feature occurrence frequencies and different binding modes over the course of a trajectory. The direct usage of these property-density functions for virtual screening would represent a true paradigm shift in 3D pharmacophore modeling.

Several advanced approaches also consider entropic effects of ligand binding for 3D pharmacophore modeling.^{71–73,78,79,81,103} PyRod, for instance, analyzes the protein environment of water molecules in MD simulations, which allows for placement of pharmacophore features at hydration sites with certain thermodynamic characteristics.⁷⁹ Such hydration sites may harbor water molecules in a highly hydrophobic protein environment or heavily restrain water molecules via hydrogen bonds and the shape of the binding pocket. The restriction of 3D pharmacophores to entropically and enthalpically important sites render such approaches valuable tools for virtual screening campaigns,

especially for those generating 3D pharmacophores from an apo structure. Importantly, PyRod is a free and open-access tool making such strategies accessible to a broader user base.

The combination of 3D pharmacophore concept and machine learning/artificial intelligence is only in its beginning stages. Although some approaches already exist,^{30,82–86} we predict an increasing number of studies and methods that aim to use pharmacophore features as descriptors or try to generate 3D pharmacophores from big data. Another trend that we observe is the availability of freely available web services for pharmacophore-based virtual screening.^{87–91}

The recent developments in the field of 3D pharmacophores are promising and afford the opportunity to employ 3D pharmacophores in ever-increasing ways and more challenging situations, such as multitarget prediction, modeling binding kinetics, or pathway-specific receptor activation. Overall, 3D pharmacophores represent an essential part of the toolbox for computer-aided drug design and are perfectly apt to identify novel ligands and understand their interaction with the macromolecular target.

ACKNOWLEDGMENTS

We thank the German Research Foundation (DFG 407626949) for financial support of M.B. We thank the Sonnenfeld Foundation for financial support of T.N. DŠ acknowledges funding from German Academic Exchange Service. We thank the China Scholarship Council (201606010328) for financial support of L.D.

CONFLICT OF INTEREST

The authors have declared no conflicts of interest for this article.

AUTHOR CONTRIBUTIONS


David Schaller: Conceptualization; visualization; writing-original draft; writing-review and editing. **Dora Sribar:** Visualization; writing-original draft; writing-review and editing. **Tessa Noonan:** Writing-original draft; writing-review and editing. **Lihua Deng:** Writing-original draft; writing-review and editing. **Trung Ngoc Nguyen:** Writing-original draft; writing-review and editing. **Szymon Pach:** Writing-original draft; writing-review and editing. **David Machalz:** Writing-original draft; writing-review and editing. **Marcel Bermudez:** Conceptualization; visualization; writing-original draft; writing-review and editing. **Gerhard Wolber:** Conceptualization; supervision; visualization; writing-original draft; writing-review and editing.

ORCID

David Schaller  <https://orcid.org/0000-0002-1881-4518>

Theresa Noonan  <https://orcid.org/0000-0003-4924-6848>

Lihua Deng  <https://orcid.org/0000-0002-7173-6897>

Trung Ngoc Nguyen  <https://orcid.org/0000-0002-7415-4390>

Szymon Pach  <https://orcid.org/0000-0001-6109-7123>

David Machalz  <https://orcid.org/0000-0001-8634-9411>

Marcel Bermudez  <https://orcid.org/0000-0002-7421-3282>

Gerhard Wolber  <https://orcid.org/0000-0002-5344-0048>

RELATED WIREs ARTICLES

[Computational chemogenomics](#)

[Computational methods for scaffold hopping](#)

[Generation of three-dimensional pharmacophore models](#)

[Computational close up on protein-protein interactions: how to unravel the invisible using molecular dynamics simulations?](#)

REFERENCES

1. Güner OF, Bowen JP. Setting the record straight: The origin of the pharmacophore concept. *J Chem Inf Model.* 2014;54(5):1269–1283. <https://doi.org/10.1021/ci5000533>
2. Reymond J-L, van Deursen R, Blum LC, Ruddigkeit L. Chemical space as a source for new drugs. *Med Chem Commun.* 2010;1(1):30. <https://doi.org/10.1039/c0md00020e>
3. Gromski PS, Henson AB, Granda JM, Cronin L. How to explore chemical space using algorithms and automation. *Nat Rev Chem.* 2019; 3(2):119–128. <https://doi.org/10.1038/s41570-018-0066-y>

4. Van Drie JH. Generation of three-dimensional pharmacophore models. *Wiley Interdis Rev.* 2013;3(5):449–464. <https://doi.org/10.1002/wcms.1129>
5. Voth AR, Khuu P, Oishi K, Ho PS. Halogen bonds as orthogonal molecular interactions to hydrogen bonds. *Nat Chem.* 2009;1(1):74–79. <https://doi.org/10.1038/nchem.112>
6. Lu Y, Shi T, Wang Y, et al. Halogen bonding—a novel interaction for rational drug design? *J Med Chem.* 2009;52(9):2854–2862. <https://doi.org/10.1021/jm9000133>
7. Wilcken R, Zimmermann MO, Lange A, Joerger AC, Boeckler FM. Principles and applications of halogen bonding in medicinal chemistry and chemical biology. *J Med Chem.* 2013;56(4):1363–1388. <https://doi.org/10.1021/jm3012068>
8. Leach AR, Gillet VJ, Lewis RA, Taylor R. Three-dimensional pharmacophore methods in drug discovery. *J Med Chem.* 2010;53(2):539–558. <https://doi.org/10.1021/jm900817u>
9. Baroni M, Cruciani G, Sciabola S, Perruccio F, Mason JS. A common reference framework for analyzing/comparing proteins and ligands. Fingerprints for ligands and proteins (FLAP): Theory and application. *J Chem Inf Model.* 2007;47(2):279–294. <https://doi.org/10.1021/ci600253e>
10. Koes DR, Camacho CJ. Pharmer: Efficient and exact pharmacophore search. *J Chem Inf Model.* 2011;51(6):1307–1314. <https://doi.org/10.1021/ci200097m>
11. Wolber G, Langer T. LigandScout: 3-D pharmacophores derived from protein-bound ligands and their use as virtual screening filters. *J Chem Inf Model.* 2005;45(1):160–169. <https://doi.org/10.1021/ci049885e>
12. Barnum D, Greene J, Smellie A, Sprague P. Identification of common functional configurations among molecules. *J Chem Inf Comput Sci.* 1996;36(3):563–571. <https://doi.org/10.1021/ci950273r>
13. Chemical Computing Group. Molecular operating environment (MOE). Montreal, QC, Canada; 2010.
14. Dixon SL, Smondryev AM, Knoll EH, Rao SN, Shaw DE, Friesner RA. PHASE: A new engine for pharmacophore perception, 3D QSAR model development, and 3D database screening: 1. Methodology and preliminary results. *J Comput Aided Mol Des.* 2006;20(10–11):647–671. <https://doi.org/10.1007/s10822-006-9087-6>
15. Taminau J, Thijs G, De Winter H. Pharao: Pharmacophore alignment and optimization. *J Mol Graph Model.* 2008;27(2):161–169. <https://doi.org/10.1016/j.jmfm.2008.04.003>
16. Certara. UNITY, SYBYL-X. St. Louis, MO; 2013.
17. Cheeseright TJ, Mackey MD, Scoffin RA. High content pharmacophores from molecular fields: A biologically relevant method for comparing and understanding ligands. *Curr Comput Aided Drug Des.* 2011;7(3):190–205. <https://doi.org/10.2174/157340911796504314>
18. Schuster D, Wolber G. Identification of bioactive natural products by pharmacophore-based virtual screening. *Curr Pharm Des.* 2010;16(15):1666–1681. <https://doi.org/10.2174/138161210791164072>
19. Wolber G, Dornhofer AA, Langer T. Efficient overlay of small organic molecules using 3D pharmacophores. *J Comput Aided Mol Des.* 2006;20(12):773–788. <https://doi.org/10.1007/s10822-006-9078-7>
20. Klebe G, Abraham U, Mietzner T. Molecular similarity indices in a comparative analysis (CoMSIA) of drug molecules to correlate and predict their biological activity. *J Med Chem.* 1994;37(24):4130–4146. <https://doi.org/10.1021/jm00050a010>
21. Cramer RD, Patterson DE, Bunce JD. Comparative molecular field analysis (CoMFA). 1. Effect of shape on binding of steroids to carrier proteins. *J Am Chem Soc.* 1988;110(18):5959–5967. <https://doi.org/10.1021/ja00226a005>
22. Friedrich N-O, de Bruyn KC, Flachsenberg F, Sommer K, Rarey M, Kirchmair J. Benchmarking commercial conformer ensemble generators. *J Chem Inf Model.* 2017;57(11):2719–2728. <https://doi.org/10.1021/acs.jcim.7b00505>
23. Spitzer GM, Wellenzohn B, Laggner C, Langer T, Liedl KR. DNA minor groove pharmacophores describing sequence specific properties. *J Chem Inf Model.* 2007;47(4):1580–1589. <https://doi.org/10.1021/ci600500v>
24. Friesner RA, Murphy RB, Repasky MP, et al. Extra precision glide: Docking and scoring incorporating a model of hydrophobic enclosure for protein-ligand complexes. *J Med Chem.* 2006;49(21):6177–6196. <https://doi.org/10.1021/jm051256o>
25. Salam NK, Nuti R, Sherman W. Novel method for generating structure-based pharmacophores using energetic analysis. *J Chem Inf Model.* 2009;49(10):2356–2368. <https://doi.org/10.1021/ci900212v>
26. Goodford PJ. A computational procedure for determining energetically favorable binding sites on biologically important macromolecules. *J Med Chem.* 1985;28(7):849–857. <https://doi.org/10.1021/jm00145a002>
27. von Itzstein M, Wu W-Y, Kok GB, et al. Rational design of potent sialidase-based inhibitors of influenza virus replication. *Nature.* 1993;363(6428):418–423. <https://doi.org/10.1038/363418a0>
28. Morris GM, Huey R, Lindstrom W, et al. AutoDock4 and AutoDockTools4: Automated docking with selective receptor flexibility. *J Comput Chem.* 2009;30(16):2785–2791. <https://doi.org/10.1002/jcc.21256>
29. Mortier J, Dhakal P, Volkamer A. Truly target-focused pharmacophore modeling: A novel tool for mapping intermolecular surfaces. *Molecules.* 2018;23(8):1959. <https://doi.org/10.3390/molecules23081959>
30. Barillari C, Marcou G, Rognan D. Hot-spots-guided receptor-based pharmacophores (HS-pharm): A knowledge-based approach to identify ligand-anchoring atoms in protein cavities and prioritize structure-based pharmacophores. *J Chem Inf Model.* 2008;48(7):1396–1410. <https://doi.org/10.1021/ci800064z>
31. Hurst T. Flexible 3D searching: The directed tweak technique. *J Chem Inf Model.* 1994;34(1):190–196. <https://doi.org/10.1021/ci00017a025>
32. Seidel T, Ibis G, Bendix F, Wolber G. Strategies for 3D pharmacophore-based virtual screening. *Drug Discov Today Technol.* 2010;7(4):e221–e228. <https://doi.org/10.1016/j.ddtec.2010.11.004>

33. Hawkins PCD. Conformation generation: The state of the art. *J Chem Inf Model*. 2017;57(8):1747–1756. <https://doi.org/10.1021/acs.jcim.7b00221>
34. Kirchmair J, Distinto S, Markt P, et al. How to optimize shape-based virtual screening: Choosing the right query and including chemical information. *J Chem Inf Model*. 2009;49(3):678–692. <https://doi.org/10.1021/ci8004226>
35. Kirchmair J, Distinto S, Schuster D, Spitzer G, Langer T, Wolber G. Enhancing drug discovery through in silico screening: Strategies to increase true positives retrieval rates. *Curr Med Chem*. 2008;15(20):2040–2053. <https://doi.org/10.2174/092986708785132843>
36. Kirchmair J, Wolber G, Laggner C, Langer T. Comparative performance assessment of the conformational model generators omega and catalyst: A large-scale survey on the retrieval of protein-bound ligand conformations. *J Chem Inf Model*. 2006;46(4):1848–1861. <https://doi.org/10.1021/ci060084g>
37. Sanders MPA, Barbosa AJM, Zarzycka B, et al. Comparative analysis of pharmacophore screening tools. *J Chem Inf Model*. 2012;52(6):1607–1620. <https://doi.org/10.1021/ci2005274>
38. Mysinger MM, Carchia M, Irwin JJ, Shoichet BK. Directory of useful decoys, enhanced (DUD-E): Better ligands and decoys for better benchmarking. *J Med Chem*. 2012;55(14):6582–6594. <https://doi.org/10.1021/jm300687e>
39. Ntie-Kang F, Simoben CV, Karaman B, et al. Pharmacophore modeling and in silico toxicity assessment of potential anticancer agents from African medicinal plants. *Drug Des Devel Ther*. 2016;10:2137–2154. <https://doi.org/10.2147/DDDT.S108118>
40. Braga RC, Andrade CH. Assessing the performance of 3D pharmacophore models in virtual screening: How good are they? *Curr Top Med Chem*. 2013;13(9):1127–1138. <https://doi.org/10.2174/1568026611313090010>
41. Triballeau N, Acher F, Brabet I, Pin J-P, Bertrand H-O. Virtual screening workflow development guided by the “receiver operating characteristic” curve approach. Application to high-throughput docking on metabotropic glutamate receptor subtype 4. *J Med Chem*. 2005;48(7):2534–2547. <https://doi.org/10.1021/jm049092j>
42. Kumar H, Kawai T, Akira S. Toll-like receptors and innate immunity. *Biochem Biophys Res Commun*. 2009;388(4):621–625. <https://doi.org/10.1016/j.bbrc.2009.08.062>
43. Murgueitio MS, Rakers C, Frank A, Wolber G. Balancing inflammation: Computational design of small-molecule toll-like receptor modulators. *Trends Pharmacol Sci*. 2017;38(2):155–168. <https://doi.org/10.1016/j.tips.2016.10.007>
44. Murgueitio MS, Henneke P, Glossmann H, Santos-Sierra S, Wolber G. Prospective virtual screening in a sparse data scenario: Design of small-molecule TLR2 antagonists. *ChemMedChem*. 2014;9(4):813–822. <https://doi.org/10.1002/cmdc.201300445>
45. Grabowski M, Murgueitio MS, Bermudez M, Rademann J, Wolber G, Weindl G. Identification of a pyrogallol derivative as a potent and selective human TLR2 antagonist by structure-based virtual screening. *Biochem Pharmacol*. 2018;154:148–160. <https://doi.org/10.1016/j.bcp.2018.04.018>
46. Grabowski M, Murgueitio MS, Bermudez M, Wolber G, Weindl G. The novel small-molecule antagonist MMG-11 preferentially inhibits TLR2/1 signaling. *Biochem Pharmacol*. 2020;171:113687. <https://doi.org/10.1016/j.bcp.2019.113687>
47. Šribar D, Grabowski M, Murgueitio MS, Bermudez M, Weindl G, Wolber G. Identification and characterization of a novel chemotype for human TLR8 inhibitors. *Eur J Med Chem*. 2019;179:744–752. <https://doi.org/10.1016/j.ejmech.2019.06.084>
48. Singh J, Petter RC, Baillie TA, Whitty A. The resurgence of covalent drugs. *Nat Rev Drug Discov*. 2011;10(4):307–317. <https://doi.org/10.1038/nrd3410>
49. De Cesco S, Kurian J, Dufresne C, Mittermaier AK, Moitessier N. Covalent inhibitors design and discovery. *Eur J Med Chem*. 2017;138:96–114. <https://doi.org/10.1016/j.ejmech.2017.06.019>
50. Johnson DS, Weerapana E, Cravatt BF. Strategies for discovering and derisking covalent, irreversible enzyme inhibitors. *Future Med Chem*. 2010;2(6):949–964. <https://doi.org/10.4155/fmc.10.21>
51. Bauer RA. Covalent inhibitors in drug discovery: From accidental discoveries to avoided liabilities and designed therapies. *Drug Discov Today*. 2015;20(9):1061–1073. <https://doi.org/10.1016/j.drudis.2015.05.005>
52. London N, Miller RM, Krishnan S, et al. Covalent docking of large libraries for the discovery of chemical probes. *Nat Chem Biol*. 2014;10(12):1066–1072. <https://doi.org/10.1038/nchembio.1666>
53. Lonsdale R, Burgess J, Colclough N, et al. Expanding the armory: Predicting and tuning covalent warhead reactivity. *J Chem Inf Model*. 2017;57(12):3124–3137. <https://doi.org/10.1021/acs.jcim.7b00553>
54. Schulz R, Atef A, Becker D, et al. Phenylthiomethyl ketone-based fragments show selective and irreversible inhibition of enteroviral 3C proteases. *J Med Chem*. 2018;61(3):1218–1230. <https://doi.org/10.1021/acs.jmedchem.7b01440>
55. Murray CW, Rees DC. The rise of fragment-based drug discovery. *Nat Chem*. 2009;1(3):187–192. <https://doi.org/10.1038/nchem.217>
56. Hauser AS, Attwood MM, Rask-Andersen M, Schiöth HB, Gloriam DE. Trends in GPCR drug discovery: New agents, targets and indications. *Nat Rev Drug Discov*. 2017;16(12):829–842. <https://doi.org/10.1038/nrd.2017.178>
57. Frandsen IO, Boesgaard MW, Fidom K, et al. Identification of histamine H3 receptor ligands using a new crystal structure fragment-based method. *Sci Rep*. 2017;7(1):4829. <https://doi.org/10.1038/s41598-017-05058-w>
58. Fidom K, Isberg V, Hauser AS, et al. A new crystal structure fragment-based pharmacophore method for G protein-coupled receptors. *Methods*. 2015;71:104–112. <https://doi.org/10.1016/j.ymeth.2014.09.009>
59. Schaller D, Hagenow S, Stark H, Wolber G. Ligand-guided homology modeling drives identification of novel histamine H3 receptor ligands. *PLoS One*. 2019;14(6):e0218820. <https://doi.org/10.1371/journal.pone.0218820>
60. Temml V, Garscha U, Romp E, et al. Discovery of the first dual inhibitor of the 5-lipoxygenase-activating protein and soluble epoxide hydrolase using pharmacophore-based virtual screening. *Sci Rep*. 2017;7(1):42751. <https://doi.org/10.1038/srep42751>

61. Waltenberger B, Garscha U, Temml V, et al. Discovery of potent soluble epoxide hydrolase (sEH) inhibitors by pharmacophore-based virtual screening. *J Chem Inf Model.* 2016;56(4):747–762. <https://doi.org/10.1021/acs.jcim.5b00592>
62. Yao T-T, Fang S-W, Li Z-S, et al. Discovery of novel succinate dehydrogenase inhibitors by the integration of in silico library design and pharmacophore mapping. *J Agric Food Chem.* 2017;65(15):3204–3211. <https://doi.org/10.1021/acs.jafc.7b00249>
63. Rakers C, Schumacher F, Meinel W, Glatt H, Kleuser B, Wolber G. In silico prediction of human sulfotransferase 1E1 activity guided by pharmacophores from molecular dynamics simulations. *J Biol Chem.* 2016;291(1):58–71. <https://doi.org/10.1074/jbc.M115.685610>
64. Tkachenko A, Bermudez M, Irmer-Stooff S, et al. Nuclear transport of the human aryl hydrocarbon receptor and subsequent gene induction relies on its residue histidine 291. *Arch Toxicol.* 2018;92(3):1151–1160. <https://doi.org/10.1007/s00204-017-2129-0>
65. Bermudez M, Rakers C, Wolber G. Structural characteristics of the allosteric binding site represent a key to subtype selective modulators of muscarinic acetylcholine receptors. *Mol Inform.* 2015;34(8):526–530. <https://doi.org/10.1002/minf.201500025>
66. Bock A, Bermudez M, Krebs F, et al. Ligand binding ensembles determine graded agonist efficacies at a G protein-coupled receptor. *J Biol Chem.* 2016;291(31):16375–16389. <https://doi.org/10.1074/jbc.M116.735431>
67. Bermudez M, Bock A, Krebs F, et al. Ligand-specific restriction of extracellular conformational dynamics constrains signaling of the M2 muscarinic receptor. *ACS Chem Biol.* 2017;12(7):1743–1748. <https://doi.org/10.1021/acschembio.7b00275>
68. Bermudez M, Bock A. Does divergent binding pocket closure drive ligand bias for class a GPCRs? *Trends Pharmacol Sci.* 2019;40(4):236–239. <https://doi.org/10.1016/j.tips.2019.02.005>
69. Bermudez M, Nguyen TN, Omieczynski C, Wolber G. Strategies for the discovery of biased GPCR ligands. *Drug Discov Today.* 2019;24(4):1031–1037. <https://doi.org/10.1016/j.drudis.2019.02.010>
70. Agnetta L, Bermudez M, Riefolo F, et al. Fluorination of photoswitchable muscarinic agonists tunes receptor pharmacology and photochromic properties. *J Med Chem.* 2019;62(6):3009–3020. <https://doi.org/10.1021/acs.jmedchem.8b01822>
71. Hu B, Lill MA. Protein pharmacophore selection using hydration-site analysis. *J Chem Inf Model.* 2012;52(4):1046–1060. <https://doi.org/10.1021/ci200620h>
72. Yu W, Lakkaraju SK, Raman EP, MacKerell AD. Site-identification by ligand competitive saturation (SILCS) assisted pharmacophore modeling. *J Comput Aided Mol Des.* 2014;28(5):491–507. <https://doi.org/10.1007/s10822-014-9728-0>
73. Yu W, Lakkaraju SK, Raman EP, Fang L, MacKerell AD. Pharmacophore modeling using site-identification by ligand competitive saturation (SILCS) with multiple probe molecules. *J Chem Inf Model.* 2015;55(2):407–420. <https://doi.org/10.1021/ci500691p>
74. Sydow D. Dynophores: Novel dynamic pharmacophores (Master Thesis). Humboldt-Universität zu Berlin; 2015.
75. Wieder M, Garon A, Perricone U, et al. Common hits approach: Combining pharmacophore modeling and molecular dynamics simulations. *J Chem Inf Model.* 2017;57(2):365–385. <https://doi.org/10.1021/acs.jcim.6b00674>
76. Perricone U, Wieder M, Seidel T, et al. A molecular dynamics-shared pharmacophore approach to boost early-enrichment virtual screening: A case study on peroxisome proliferator-activated receptor α . *ChemMedChem.* 2017;12(16):1399–1407. <https://doi.org/10.1002/cmdc.201600526>
77. Schuetz DA, Seidel T, Garon A, et al. GRAIL: Grids of pharmacophore interaction fields. *J Chem Theory Comput.* 2018;14(9):4958–4970. <https://doi.org/10.1021/acs.jctc.8b00495>
78. Jung SW, Kim M, Ramsey S, Kurtzman T, Cho AE. Water pharmacophore: Designing ligands using molecular dynamics simulations with water. *Sci Rep.* 2018;8(1):1–11. <https://doi.org/10.1038/s41598-018-28546-z>
79. Schaller D, Pach S, Wolber G. PyRod: Tracing water molecules in molecular dynamics simulations. *J Chem Inf Model.* 2019;59(6):2818–2829. <https://doi.org/10.1021/acs.jcim.9b00281>
80. Arcon JP, Modenutti CP, Avendaño D, et al. AutoDock bias: Improving binding mode prediction and virtual screening using known protein-ligand interactions. Cowen L, editor. *Bioinformatics.* 2019;35(19):3836–3838. <https://doi.org/10.1093/bioinformatics/btz152>
81. Lee JY, Krieger JM, Li H, Bahar I. Pharmmaker: Pharmacophore modeling and hit identification based on druggability simulations. *Protein Sci.* 2020;29(1):76–86. <https://doi.org/10.1002/pro.3732>
82. Sato T, Honma T, Yokoyama S. Combining machine learning and pharmacophore-based interaction fingerprint for in silico screening. *J Chem Inf Model.* 2010;50(1):170–185. <https://doi.org/10.1021/ci900382e>
83. Jiménez J, Doerr S, Martínez-Rosell G, Rose AS, De Fabritiis G. DeepSite: Protein-binding site predictor using 3D-convolutional neural networks. Valencia a, editor. *Bioinformatics.* 2017;33(19):3036–3042. <https://doi.org/10.1093/bioinformatics/btx350>
84. Jiménez J, Škalič M, Martínez-Rosell G, De Fabritiis G. K DEEP: Protein-ligand absolute binding affinity prediction via 3D-convolutional neural networks. *J Chem Inf Model.* 2018;58(2):287–296. <https://doi.org/10.1021/acs.jcim.7b00650>
85. Škalič M, Varela-Rial A, Jiménez J, Martínez-Rosell G, De Fabritiis G. LigVoxel: Inpainting binding pockets using 3D-convolutional neural networks. Valencia a, editor. *Bioinformatics.* 2019;35(2):243–250. <https://doi.org/10.1093/bioinformatics/bty583>
86. Škalič M, Jiménez J, Sabbadin D, De Fabritiis G. Shape-based generative modeling for de novo drug design. *J Chem Inf Model.* 2019;59(3):1205–1214. <https://doi.org/10.1021/acs.jcim.8b00706>
87. Schneidman-Duhovny D, Dror O, Inbar Y, Nussinov R, Wolfson HJ. PharmaGist: A webserver for ligand-based pharmacophore detection. *Nucleic Acids Res.* 2008;36:W223–W228. <https://doi.org/10.1093/nar/gkn187>
88. Wang X, Shen Y, Wang S, et al. PharmMapper 2017 update: A web server for potential drug target identification with a comprehensive target pharmacophore database. *Nucleic Acids Res.* 2017;45(W1):W356–W360. <https://doi.org/10.1093/nar/gkx374>
89. Sunseri J, Koes DR. Pharmit: Interactive exploration of chemical space. *Nucleic Acids Res.* 2016;44(W1):W442–W448. <https://doi.org/10.1093/nar/gkw287>

90. Koes D, Khoury K, Huang Y, et al. Enabling large-scale design, synthesis and validation of small molecule protein-protein antagonists. *PLoS One*. 2012;7(3):e32839. <https://doi.org/10.1371/journal.pone.0032839>
91. Koes DR, Camacho CJ. ZINCPharmer: Pharmacophore search of the ZINC database. *Nucleic Acids Res*. 2012;40(W1):W409–W414. <https://doi.org/10.1093/nar/gks378>
92. Carlson HA, Masukawa KM, Rubins K, et al. Developing a dynamic pharmacophore model for HIV-1 integrase. *J Med Chem*. 2000;43(11):2100–2114. <https://doi.org/10.1021/jm990322h>
93. Damm KL, Carlson HA. Exploring experimental sources of multiple protein conformations in structure-based drug design. *J Am Chem Soc*. 2007;129(26):8225–8235. <https://doi.org/10.1021/ja0709728>
94. Guvench O, MacKerell AD. Computational fragment-based binding site identification by ligand competitive saturation. Jacobson MP, editor. *PLoS Comput Biol*. 2009;5(7):e1000435. <https://doi.org/10.1371/journal.pcbi.1000435>
95. Lanning ME, Yu W, Yap JL, et al. Structure-based design of N-substituted 1-hydroxy-4-sulfamoyl-2-naphthoates as selective inhibitors of the Mcl-1 oncoprotein. *Eur J Med Chem*. 2016;113:273–292. <https://doi.org/10.1016/j.ejmech.2016.02.006>
96. Nizami B, Sydow D, Wolber G, Honarparvar B. Molecular insight on the binding of NNRTI to K103N mutated HIV-1 RT: Molecular dynamics simulations and dynamic pharmacophore analysis. *Mol Biosyst*. 2016;12(11):3385–3395. <https://doi.org/10.1039/C6MB00428H>
97. Mortier J, Prévost JRC, Sydow D, et al. Arginase structure and inhibition: Catalytic site plasticity reveals new modulation possibilities. *Sci Rep*. 2017;7(1):13616. <https://doi.org/10.1038/s41598-017-13366-4>
98. Bergant K, Janežič M, Valjavec K, et al. Structure-guided optimization of 4,6-substituted-1,3,5-triazin-2(1H)-ones as catalytic inhibitors of human DNA topoisomerase II α . *Eur J Med Chem*. 2019;175:330–348. <https://doi.org/10.1016/j.ejmech.2019.04.055>
99. Durairaj P, Fan L, Machalz D, Wolber G, Bureik M. Functional characterization and mechanistic modeling of the human cytochrome P450 enzyme CYP4A22. *FEBS Lett*. 2019;593(16):2214–2225. <https://doi.org/10.1002/1873-3468.13489>
100. Naß A, Schaller D, Wolber G. Assessment of flexible shape complementarity: New opportunities to explain and induce selectivity in ligands of protein tyrosine phosphatase 1B. *Mol Inform*. 2019;38(5):1800141. <https://doi.org/10.1002/minf.201800141>
101. Vitorović-Todorović MD, Worek F, Perdih A, Bauk ŠD, Vujatović TB, Cvijetić IN. The in vitro protective effects of the three novel nanomolar reversible inhibitors of human cholinesterases against irreversible inhibition by organophosphorous chemical warfare agents. *Chem Biol Interact*. 2019;309:108714. <https://doi.org/10.1016/j.cbi.2019.06.027>
102. Seco J, Luque FJ, Barril X. Binding site detection and druggability index from first principles. *J Med Chem*. 2009;52(8):2363–2371. <https://doi.org/10.1021/jm801385d>
103. Arcon JP, Defelipe LA, Lopez ED, et al. Cosolvent-based protein pharmacophore for ligand enrichment in virtual screening. *J Chem Inf Model*. 2019;59(8):3572–3583. <https://doi.org/10.1021/acs.jcim.9b00371>
104. Bakan A, Nevins N, Lakdawala AS, Bahar I. Druggability assessment of allosteric proteins by dynamics simulations in the presence of probe molecules. *J Chem Theory Comput*. 2012;8(7):2435–2447. <https://doi.org/10.1021/ct300117j>
105. Amaro RE, Baudry J, Chodera J, et al. Ensemble docking in drug discovery. *Biophys J*. 2018;114(10):2271–2278. <https://doi.org/10.1016/j.bpj.2018.02.038>
106. Korb O, Olsson TSG, Bowden SJ, et al. Potential and limitations of ensemble docking. *J Chem Inf Model*. 2012;52(5):1262–1274. <https://doi.org/10.1021/ci2005934>
107. Evangelista Falcon W, Ellingson SR, Smith JC, Baudry J. Ensemble docking in drug discovery: How many protein configurations from molecular dynamics simulations are needed to reproduce known ligand binding? *J Phys Chem B*. 2019;123(25):5189–5195. <https://doi.org/10.1021/acs.jpcc.8b11491>
108. Vamathevan J, Clark D, Czodrowski P, et al. Applications of machine learning in drug discovery and development. *Nat Rev Drug Discov*. 2019;18(6):463–477. <https://doi.org/10.1038/s41573-019-0024-5>
109. Sterling T, Irwin JJ. ZINC 15—Ligand discovery for everyone. *J Chem Inf Model*. 2015;55(11):2324–2337. <https://doi.org/10.1021/acs.jcim.5b00559>
110. Gaulton A, Hersey A, Nowotka M, et al. The ChEMBL database in 2017. *Nucleic Acids Res*. 2017;45(D1):D945–D954. <https://doi.org/10.1093/nar/gkw1074>
111. Kim S, Chen J, Cheng T, et al. PubChem 2019 update: Improved access to chemical data. *Nucleic Acids Res*. 2019;47(D1):D1102–D1109. <https://doi.org/10.1093/nar/gky1033>

How to cite this article: Schaller D, Šribar D, Noonan T, et al. Next generation 3D pharmacophore modeling. *WIREs Comput Mol Sci*. 2020;10:e1468. <https://doi.org/10.1002/wcms.1468>